Seismic anisotropy of the lithospheric mantle beneath Marie Byrd Land, West Antarctica: Constraints from peridotite xenoliths

Seth C. Kruckenberg[1], Vasileios Chatzaras[2]

[1]Department of Earth & Environmental Sciences, Boston College; [2]School of Geosciences, The University fo Sydney

1. BACKGROUND

Constraining the seismic structure of the West Antarctic mantle is important for: 1) unravelling the dynamics of intracontinental extension within the West Antarctic Rift System (WARS), one of the biggest rift systems on Earth; and 2) for mapping the 3D viscosity structure of the upper mantle, required to accurately model the interaction between mantle dynamics and the West Antarctic ice sheet evolution, manifested by the glacial isostatic adjustment process.

This study is an effort to provide insights into the evolution of the subcontinental lithospheric mantle beneath the WARS, and understand how different mantle rock properties affect seismic velocities and anisotropy.

2. UPPER MANTLE XENOLITHS FROM MARIE BYRD LAND

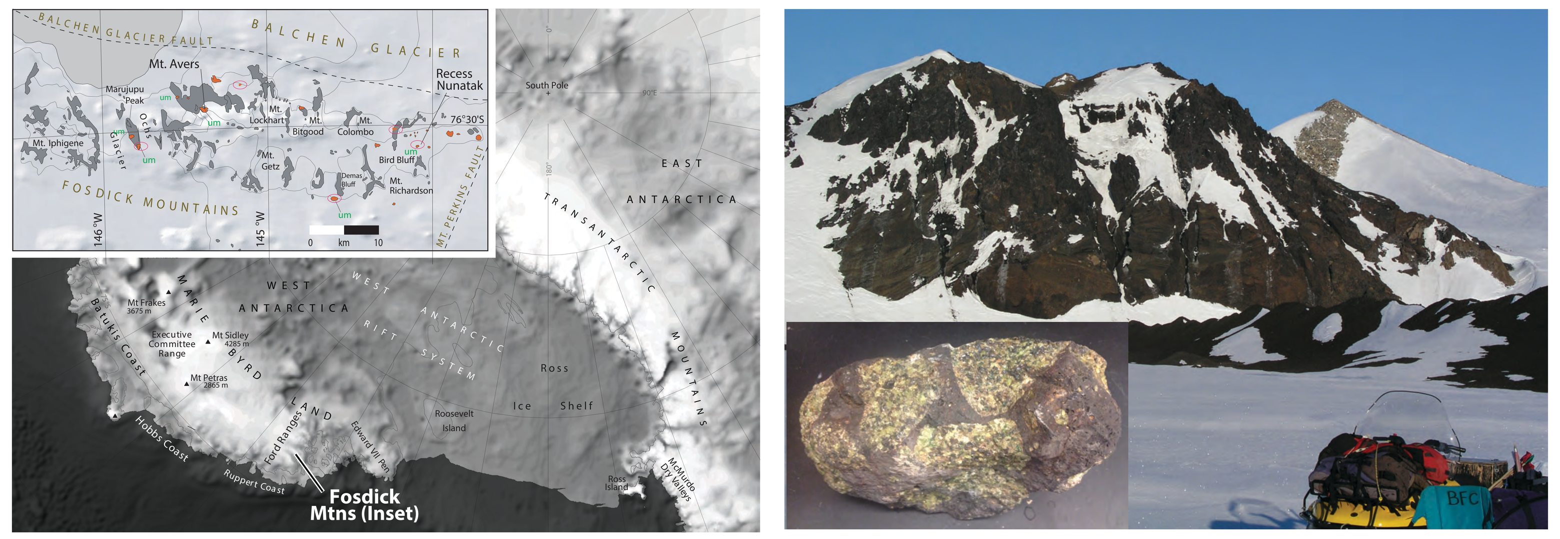

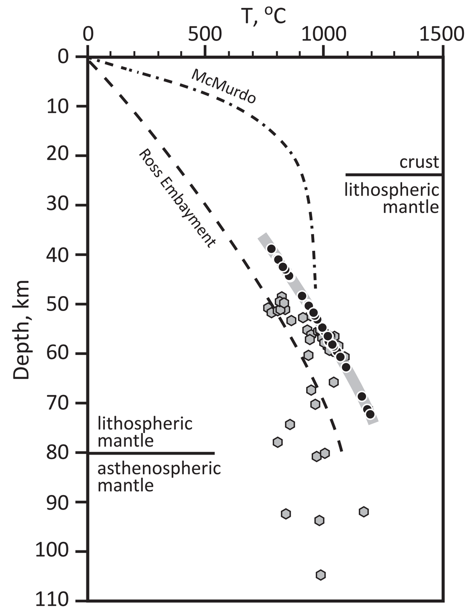

Map of Antarctica showing major geographic features in relationship to the location of studied xenolith localities in the Fosdick Mountains (inset) and the Executive Committee Range. Inset shows individual volcanic rock exposures within the Fosdick Mountains in orange. Sites with abundant ultramafic xenolites are labeled "um". Volcanic vent bearing crustal xenoliths are indicated in pink. After Gaffney & Siddoway (2007).

We analyzed 42 mantle xenoliths sampled from seven volcanic centres in western and central Marie Byrd Land (MBL); five centres are located in the Fosdick Mountains (Marujupu Peak, Mount Avers, Demas Bluff, Bird Bluff, and Recess Nunatak), one in the USAS Escarpment (Mount Aldaz) and one in the Executive Committee Range (Mount Cumming).

The average **equilibration temperatures** of the MBL xenoliths estimated from two-pyroxene geothermometers range from **780 to 1200°C**, calculated at a pressure of 15 kbar (Chatzaras et al., 2016).

3. MODAL COMPOSITION

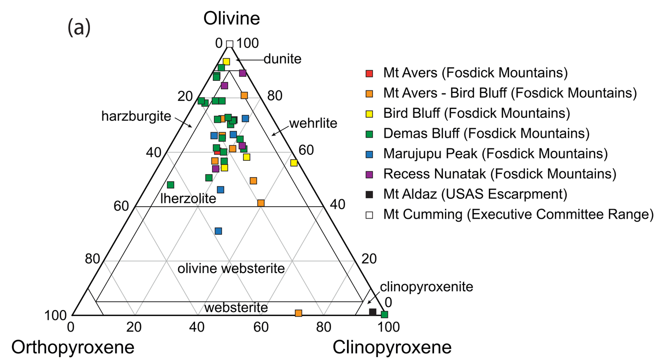

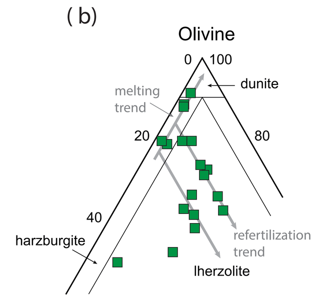

The xenoliths are classified as predominantly **lherzolites** (n=30), with lesser occurrences of **harzburgite** (n=4), **wehrlite** (n=3), **dunite** (n=3), **olivine websterite** (n=1), **websterite** (n=1), and **clinopyroxenite** (n=2). The Marie Byrd Land xenoliths are fertile, having average modal compositions of 55-71% olivine, 13-23% orthopyroxene, 15-24% clinopyroxene, and 1-2% spinel.

4. MINERAL MAJOR ELEMENT COMPOSITION

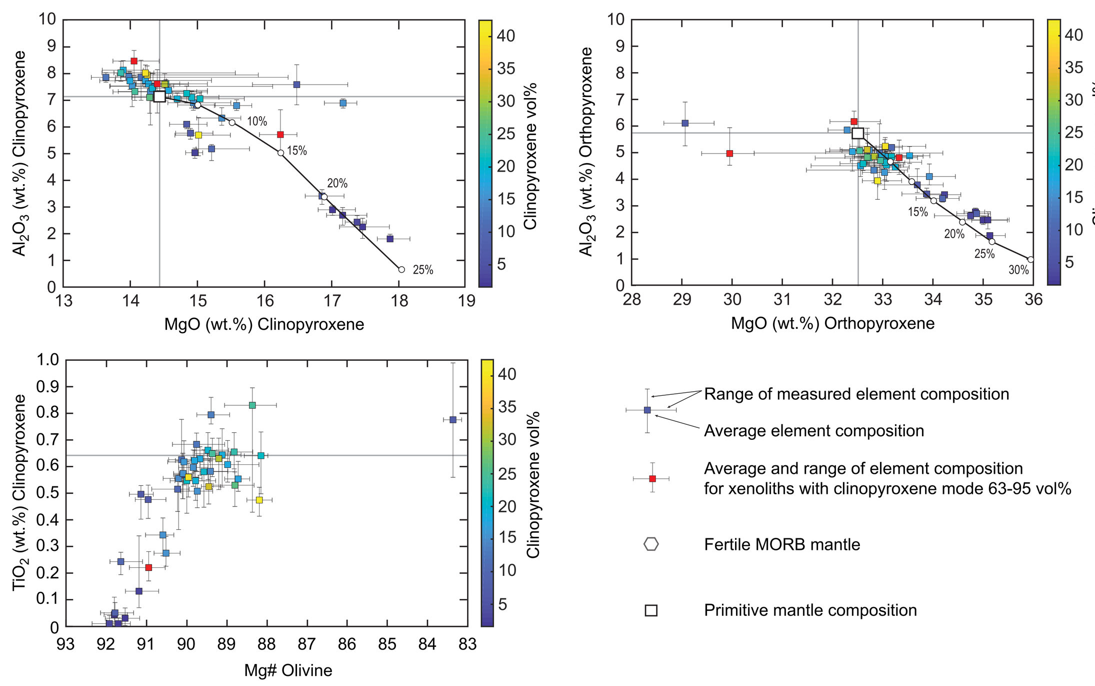

Clinopyroxenes with high Al_2O_3, Na_2O, and TiO_2, and low MgO content in a fertile group of lherzolites, wehrlites, websterites, and clinopyroxenites, may indicate refertilization.

The discrepancy in the estimated degrees of partial melting for the two pyroxenes, implies that **partial melting may not be the only process that influenced their Al_2O_3 and MgO content**.

Clinopyroxenes in the more fertile lherzolites and wehrlites show constant TiO_2 concentration at 0.65 wt% and 0.8 wt% over a range of olivine Mg# values. The observed trend is interpreted to indicate a refertilization process (Le Roux et al., 2007; Embey-Isztin, 2016).

5. MICROSTRUCTURES

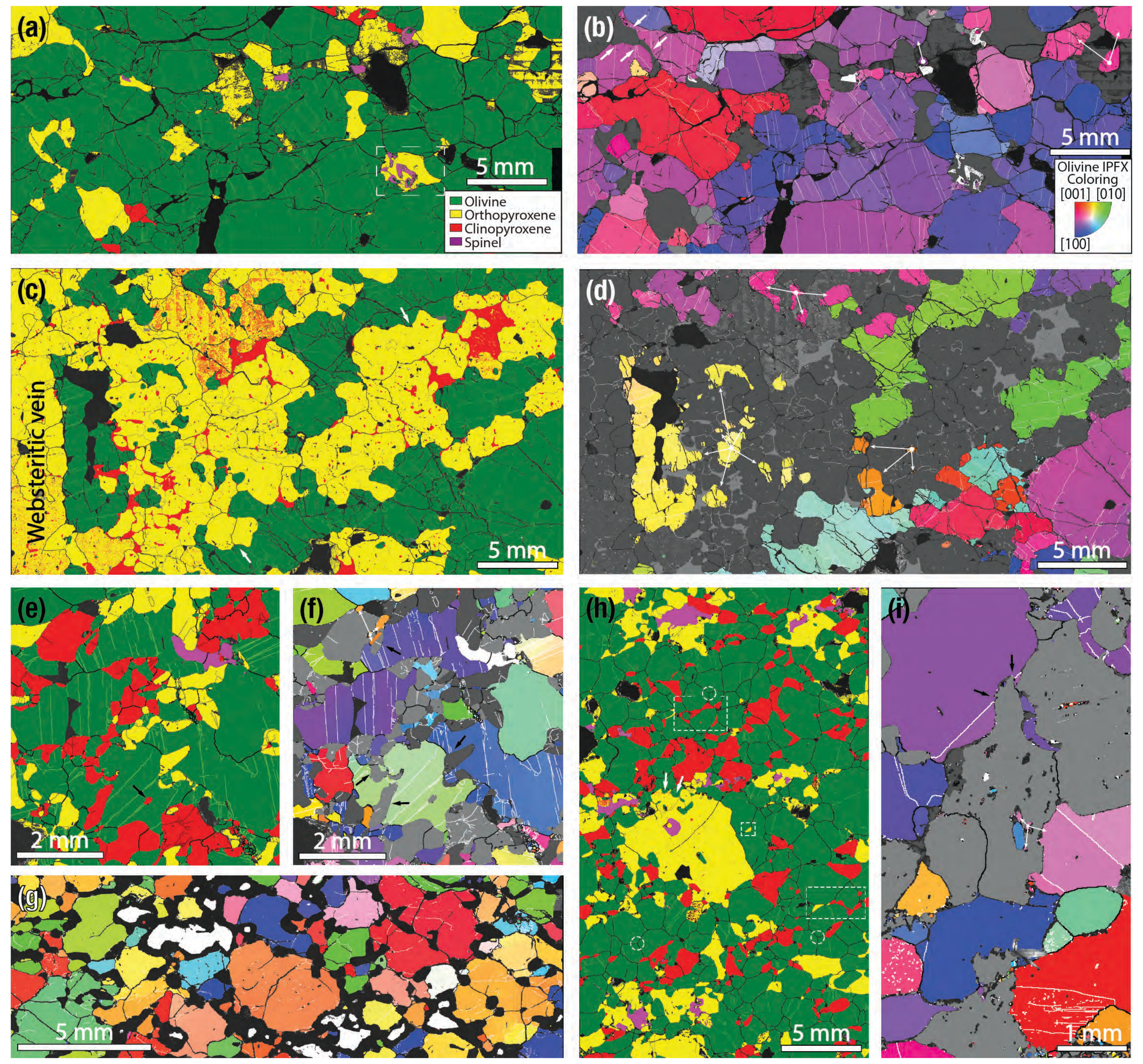

Representative EBSD phase maps and inverse pole figure (IPFX) maps.

Microstructures indicate refertilization of the MBL upper mantle as a result of reaction with percolating melts:

1) Secondary origin of pyroxenes, suggested by the occurrence of subidiomorphic to xenomorphic grains with interstitial habit that either exhibit a cuspate shape in olivine triple junctions or form film-like elongated grains along grain boundaries (Fig. c, h).

2) Occurrence of pyroxene grains that contain olivine inclusions with crystallographic orientation similar to the neighbouring olivine grains (Fig. d, f, i).

3) Formation of websteritic veins in dunite (Fig. c).

All maps have upper edge parallel to the long axis (lineation) of the spinel shape fabric ellipsoid determined using X-ray computed tomography (Chatzaras et al., 2016) with the foliation normal to the map.

All the inverse pole figure maps of olivine and clinopyroxene crystallographic axis orientations are colored relative to the spinel lineation (IPF-X coloring).

In the phase maps, phase coloring is as follows: green, olivine; yellow, orthopyroxene; red, clinopyroxene; purple, spinel.

In the combined EBSD phase and IPFX maps, phase coloring is as follows: white, spinel; light grey, clinopyroxene; and dark grey, orthopyroxene.

In both the EBSD phase maps and the combined phase and IPFX maps, black lines correspond to grain boundaries and black areas to zero solutions (not-indexed domains).

.

6. OLIVINE, ORTHOPYROXENE, AND CLINOPYROXENE CRYSTALLOGRAPHIC PREFERRED ORIENTATIONS (CPOs)

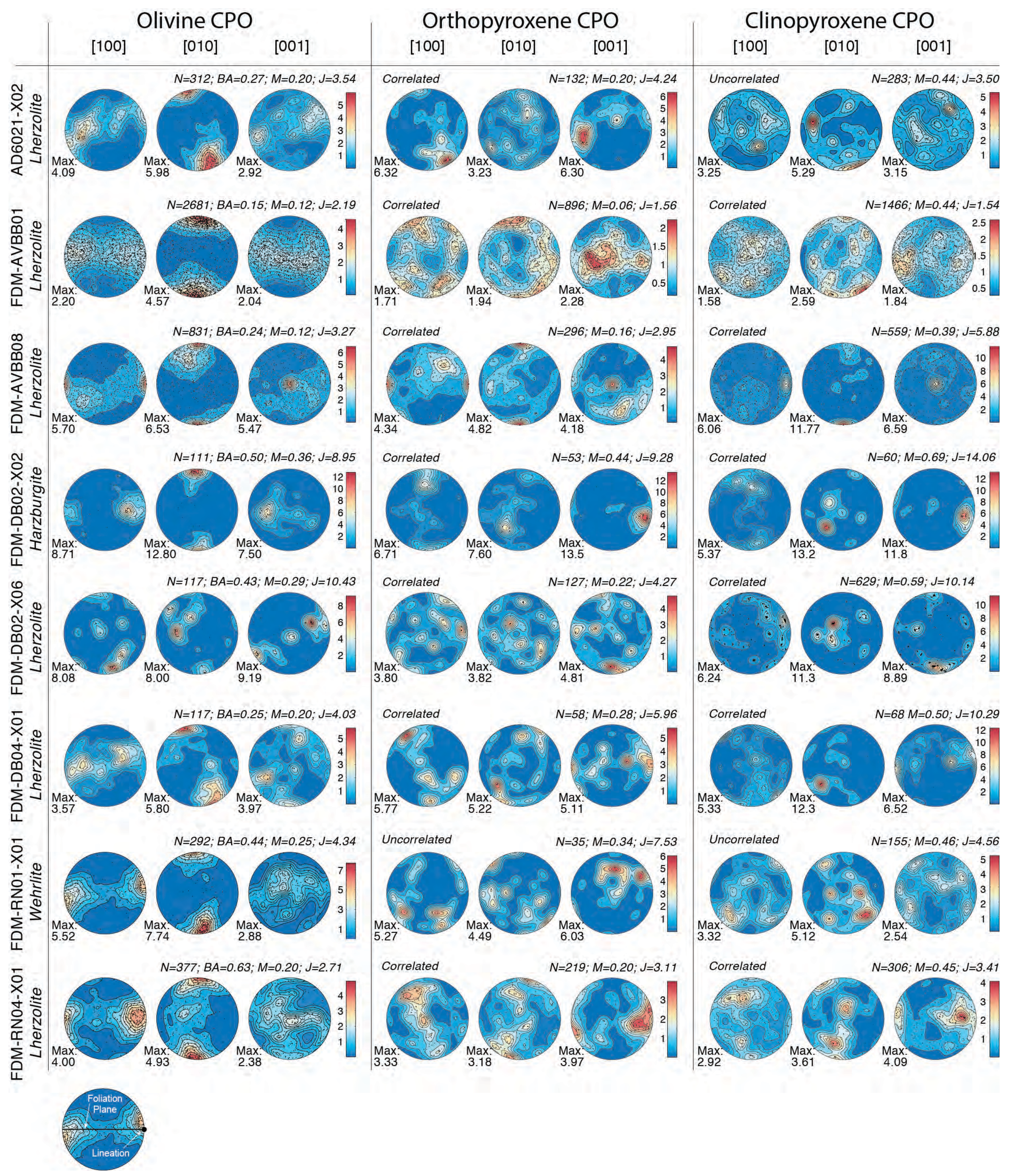

Representative CPOs of the main rock forming minerals.

The relationship between the olivine and pyroxenes CPOs can provide important constraints on the relative timing of deformation and pyroxenes crystallization from the percolating melts. Our observations suggest diachronous melt percolation in the upper mantle beneath MBL, relative to the deformation event that generated the olivine CPO.

Correlated olivine and pyroxenes CPOs suggests coherent and synchronous deformation in the three mineral phases and implies that the pyroxene grains either have a primary origin, or crystallized from melts that were transported through the upper mantle prior or at the early stages of the deformation phase that formed the olivine and pyroxenes CPOs.

Correlated olivine-orthopyroxene CPO, and uncorrelated olivine-clinopyroxene CPO imply coherent deformation of olivine and orthopyroxene, and post-deformation crystallization of clinopyroxene.

Uncorrelated olivine and pyroxenes CPOs are interpreted to show post-deformation melt percolation and pyroxene precipitation.

Crystallographic orientations are plotted as one point per grain data sets in lower hemisphere equal area projections, relative to the spinel fabric ellipsoid axes. Color scales are for multiples of uniform distribution. For each analysed mineral in a sample, the number of grains analysed, as well the M, and J indices, are given, in addition to the BA index for olivine.

7. SEISMIC ANISOTROPY

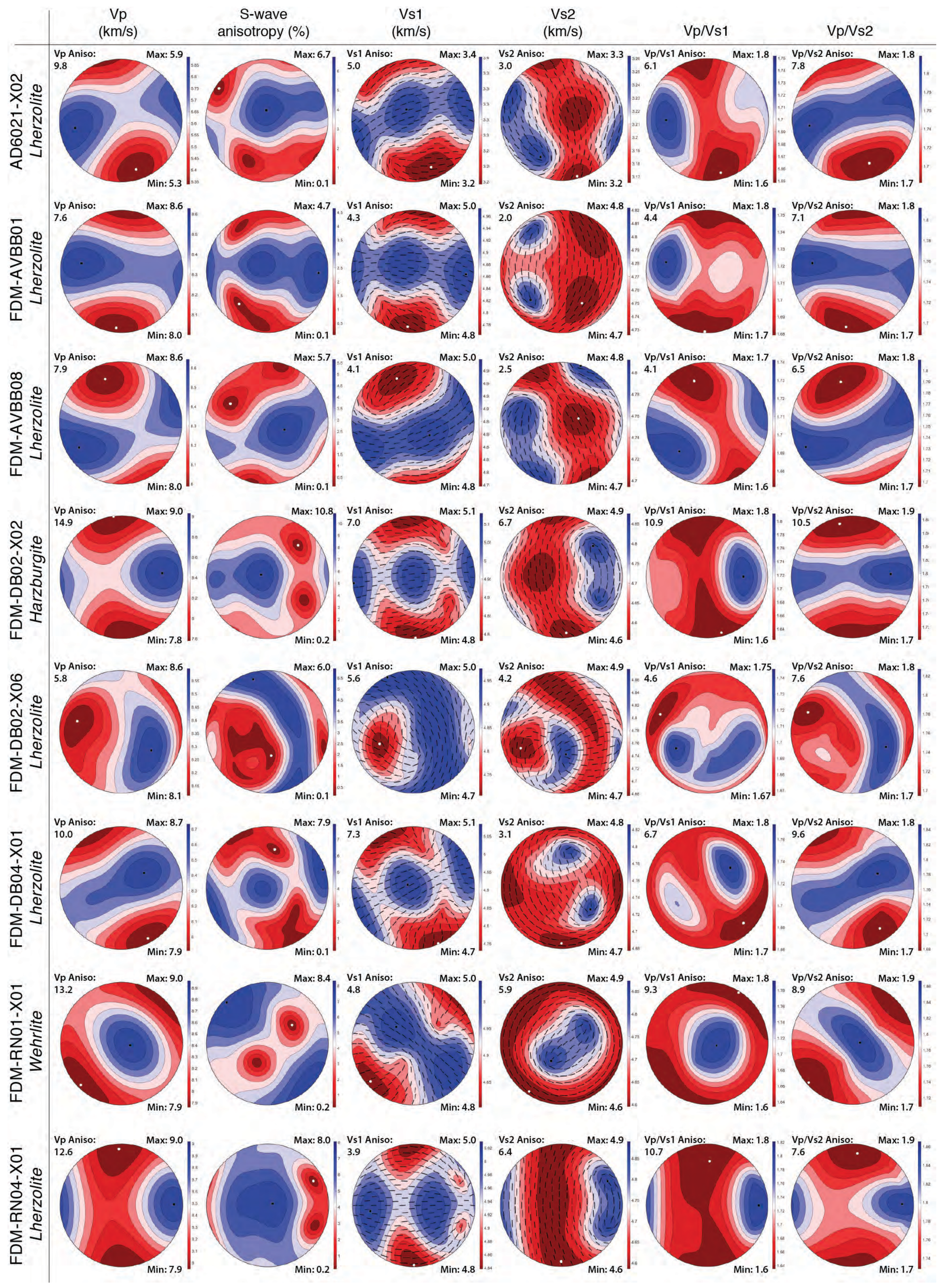

Calculated P and S waves anisotropy shows significant range of values (2–15%). Anisotropy increases with olivine mode and decreases with increasing orthopyroxene and clinopyroxene content.

P-wave anisotropy is primarily correlated with the strength of olivine CPO expressed with the M-index. It increases with increasing strength of the orthopyroxene CPO, but seems to be less correlated with the strength of the clinopyroxene CPO.

Reactive melt percolation and refertilization of the MBL upper mantle may have led to a decrease in both the P-wave and S-wave anisotrpy.

ACKNOWLEDGMENTS

We thank the United States Polar Rock Repository, Christine Siddoway and Kurt Panter for providing us with xenolith samples. This research was supported by NSF-ANT 1246320 grant to S.C. Kruckenberg. Chatzaras acknowledges support from the University of Sydney.

REFERENCES

Chatzaras, V., S. C. Kruckenberg,S. M. Cohen, L. G. Medaris Jr.,A. C. Withers, and B. Bagley (2016), Axial-type olivine crystallographicpreferred orientations: The effect ofstrain geometry on mantle texture,J. Geophys. Res. Solid Earth, 121,4895–4922, doi:10.1002/2015JB012628.

Gaffney, A. M., and C. S. Siddoway (2007), Heterogeneous sources for Pleis- tocene lavas of Marie Byrd Land, Antarctica: New Data from the SW Pacific Diffuse Alkaline Magmatic Province. In Antarctica: A Keystone in a Changing World—Online Proceedings for the Tenth International Symposium on Antarctic Earth Sciences, eds. Cooper, A. K., C. R. Raymond et al., USGS Open-File Report 2007-1047, Extended abstract 063, http://pubs.usgs.gov/of/2007/1047/.